Supporting Information

On the role of protective surface coatings on the thermal stability of delithiated Ni-rich layered oxide cathode materials

Friederike Reissig, Joaquin Ramirez-Rico, Tobias Placke, Martin Winter, Richard Schmuch[*], *Aurora Gomez-Martin*[*]

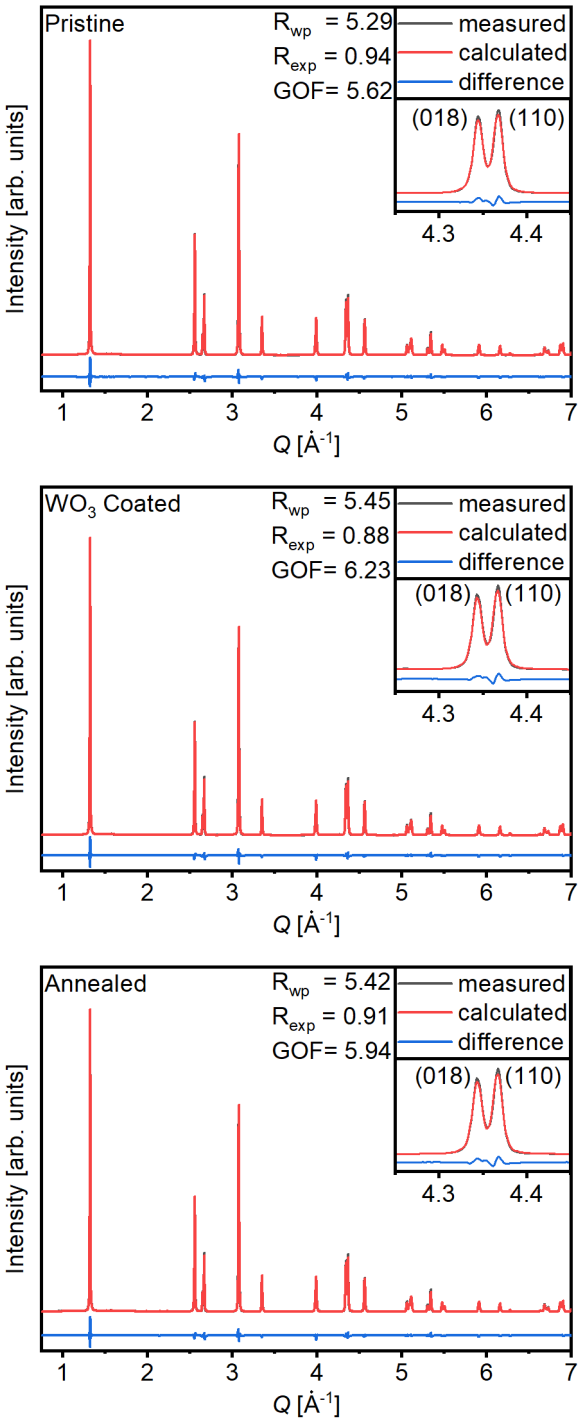

Figure S1. Rietveld refinements of the NCM materials showing measured (grey), calculated (red) data as well as the difference between them (blue). R_{wp}, R_{exp} and goodness of fit (GOF) are shown as well. The inlayer shows the (108)/(110) reflections split up indicating a well-defined layered structure.

Table S1. Information on the structural parameters used for the refinement as well as introduction of the refined parameters *z*(O), Li_{mix}, beq(O) and beq(TM).

Atom	Wyckoff Site	*x* or *a*	*y* or *b*	*z* or *c*	Occupancy	Isotropic thermal factor beq
O	*6c*	0	0	z (O)	1	beq(O)
Li1	*3a*	0	0	0	1.00– Li_{mix}	2
Ni2	*3a*	0	0	0	Li_{mix}	2
Ni1	*3b*	0	0	0.5	0.90 - Li_{mix}	beq(TM)
Co1	*3b*	0	0	0.5	0.05	beq(TM)
Mn1	*3b*	0	0	0.5	0.05	beq(TM)
Li2	*3b*	0	0	0.5	Li_{mix}	beq(TM)

Table S2. Results of the Rietveld refinements: R-weighted pattern (R_{wp}), R expected (R_{exp}), goodness of fit (GOF), lattice parameters *a* and *c*, unit cell volume (*V*), Li - Ni mixing (Li_{mix}), *z*-Position and isotropic thermal factors. (beq)

Modification	Pristine		WO_3 Coated		Annealed	
R_{wp}	5.29		5.45		5.42	
R_{exp}	0.94		0.88		0.91	
GOF	5.62		6.23		5.94	
	Main phase	Secondary phase	Main phase	Secondary phase	Main phase	Secondary phase
Percentage	66.26	28.26	71.87	22.11	71.74	22.33
***a* [10^{-10}m]**	2.8760(5)	2.8777(9)	2.8761(5)	2.878(1)	2.8766(5)	2.878(1)
***c* [10^{-10}m]**	14.204(2)	14.201(6)	14.206(2)	14.201(7)	14.209(2)	14.202(7)
***V* [$10^{-30}m^3$]**	101.75(4)	101.85(7)	101.77(4)	101.88(9)	101.82(4)	101.92(9)
c/a	4.9388	4.9348	4.9396	4.934	4.9397	4.9339
Li_{mix}	0.0393 ± 0.0005		0.0350 ± 0.0006		0.0345 ± 0.0006	
Li - Ni mixing [%]	3.93 ± 0.05		3.50 ± 0.06		3.45 ± 0.06	
***z* (O)**	0.242(1)	0.239(3)	0.242(1)	0.237(4)	0.242(1)	0.238(4)
beq(O)	0.9(1)		0.9(1)		0.9(1)	
beq(TM)	0.34(2)		0.36(2)		0.35(9)	

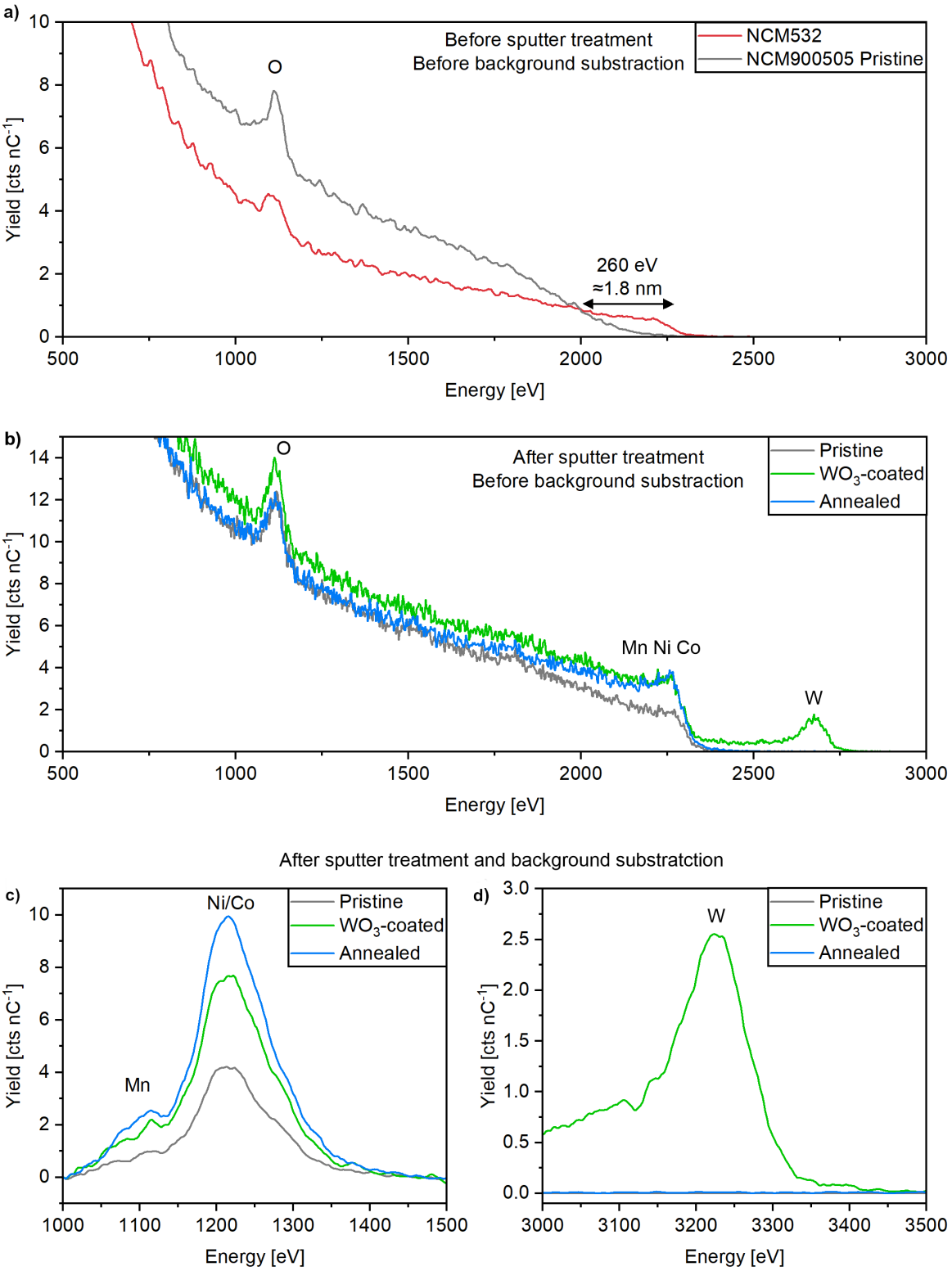

Figure S2. LEIS results. (**a**) Comparison of 3 keV $^{4}He^{+}$ spectra for the pristine sample and an NCM532 reference before the sputter treatment. The difference in background indicates a thick layer of surface residues. (**b**) 3 keV $^{4}He^{+}$ spectra for the samples in set 2 after the sputter treatment. (**c, d**) 5 keV $^{20}Ne^{+}$ spectra after background subtraction and smoothing. (**c**) Mn/Co/Ni region and d) W region.

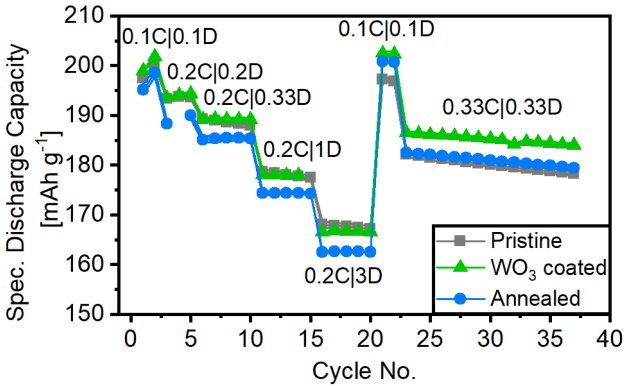

Figure S3. Rate capability investigations in NCM || Li metal cells. Specific discharge capacity vs. cycle number. Cell voltage range: 2.9 - 4.3 V (1C = 190 mA g^{-1}). Error bars: standard deviation of three cells for each sample. The missing data point in cycle 4 for the annealed sample resulted from a short power outage. 1 C=190 mA g^{-1}.

Table S3. Results of long-term stability investigation in NCM || graphite full-cells. The given errors are the standard deviation of three cells per sample.

	Initial Coulombic efficiency [%]	Initial discharge capacity at 0.1 C after formation [mAh g^{-1}]	Initial discharge capacity at 0.33 C [mAh g^{-1}]	End of life (<80% SOH) reached in cycle:
Pristine	85.80 ± 0.04	193.91 ± 0.03	186.05 ± 0.03	163
WO_3 Coated	85.9 ± 0.3	192 ± 1	184 ± 1	344
Annealed	84.0 ± 0.2	190.3 ± 0.1	180 ± 1	328

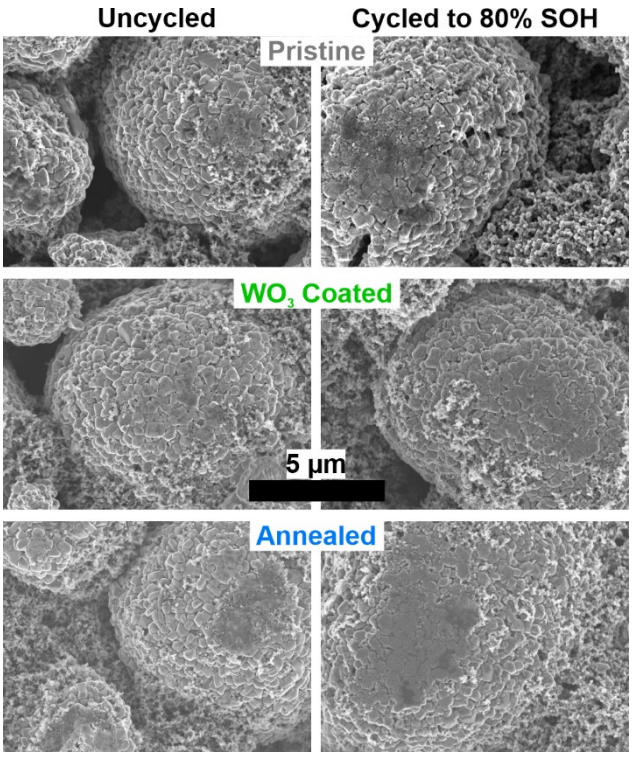

Figure S4. SEM images with a magnification of 10kx of various electrodes before (left) and after (right) cycling until 80% SOH was reached.

Table S4. Results of the differential scanning calorimetry of cathode materials delithiated to $Li_{0.31}Ni_{0.90}Co_{0.05}Mn_{0.05}O_2$. Integrated specific heat flow without and with fresh electrolyte.

Integrated heat flow [W K g^{-1}]	Without electrolyte	With fresh electrolyte
Pristine	353.5	81.8
WO_3-coated	250.9	72.0
Annealed	214.5	92.1

Table S5. Results of the differential scanning calorimetry of cathode materials delithiated to $Li_{0.31}Ni_{0.90}Co_{0.05}Mn_{0.05}O_2$. Temperatures for the position of the first peak max and where the decomposition onset of 0.2 W g^{-1} for the specific heat flow is exceeded.

	Position 1st maximum [°C]	Onset T [°C] (spec. heat flow > 0.2 W g^{-1})
Pristine	206	192
WO_3-coated	208 and 212	199
Annealed	208	190

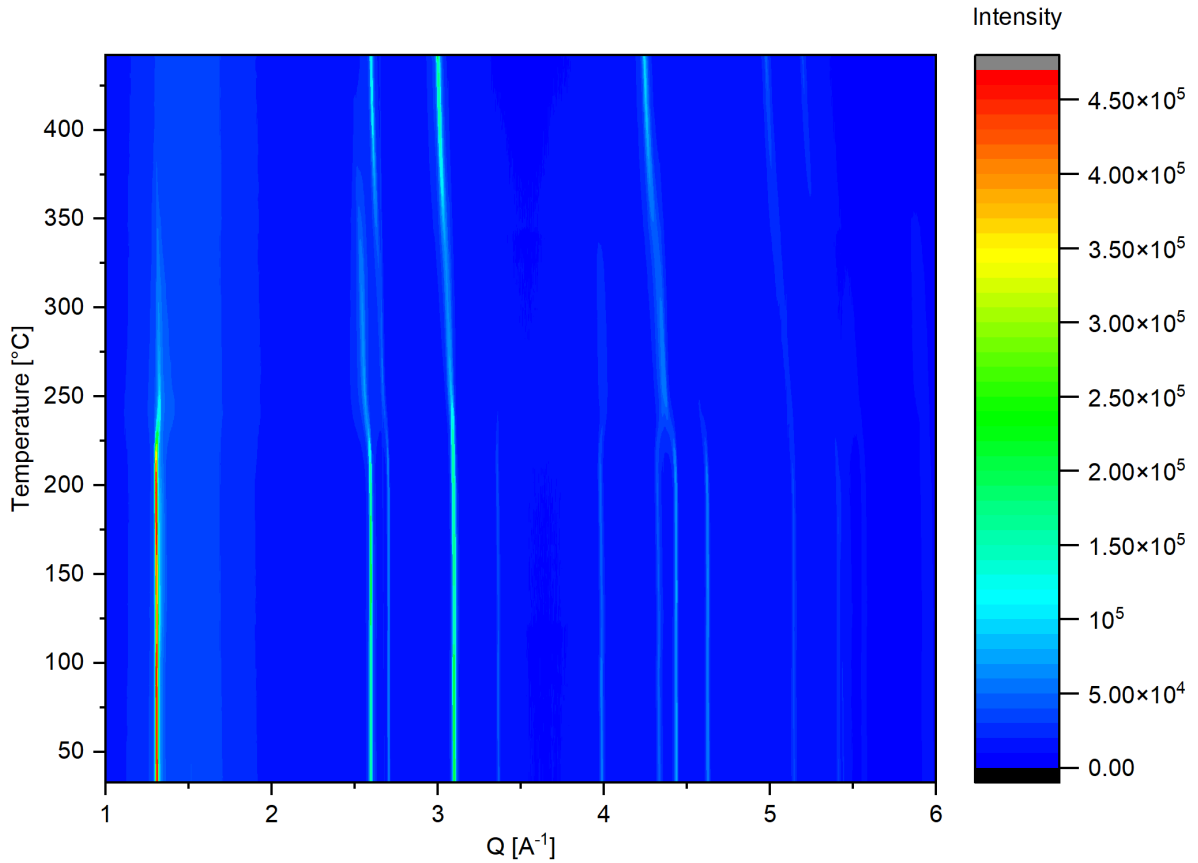

Figure S5. Diffraction pattern contour plot of the delithiated pristine material. Cathode powders in a quartz capillary were heated from room temperature to 400ºC using the ITQ-ALBA capillary flow reaction cell.

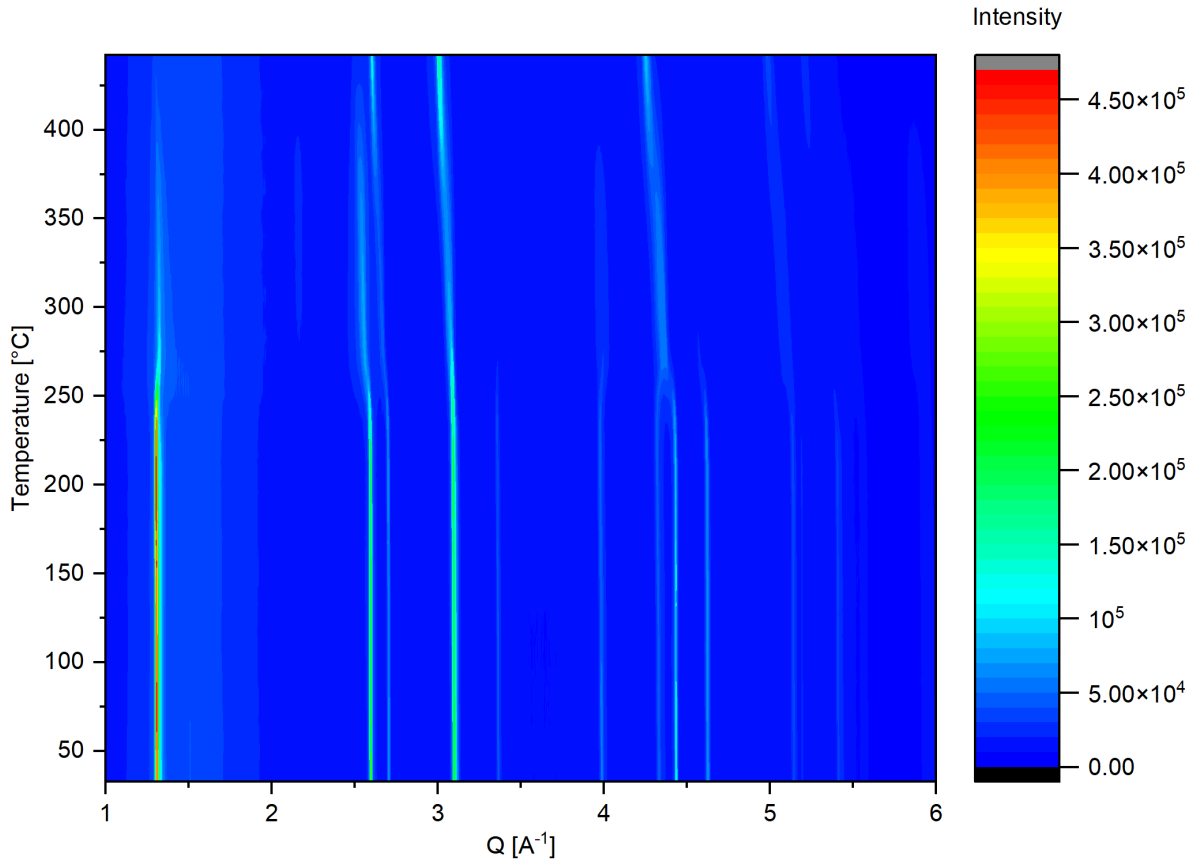

Figure S6. Diffraction pattern contour plot of delithiated WO_3-coated material. Cathode powders in a quartz capillary were heated from room temperature to 400ºC using the ITQ-ALBA capillary flow reaction cell.

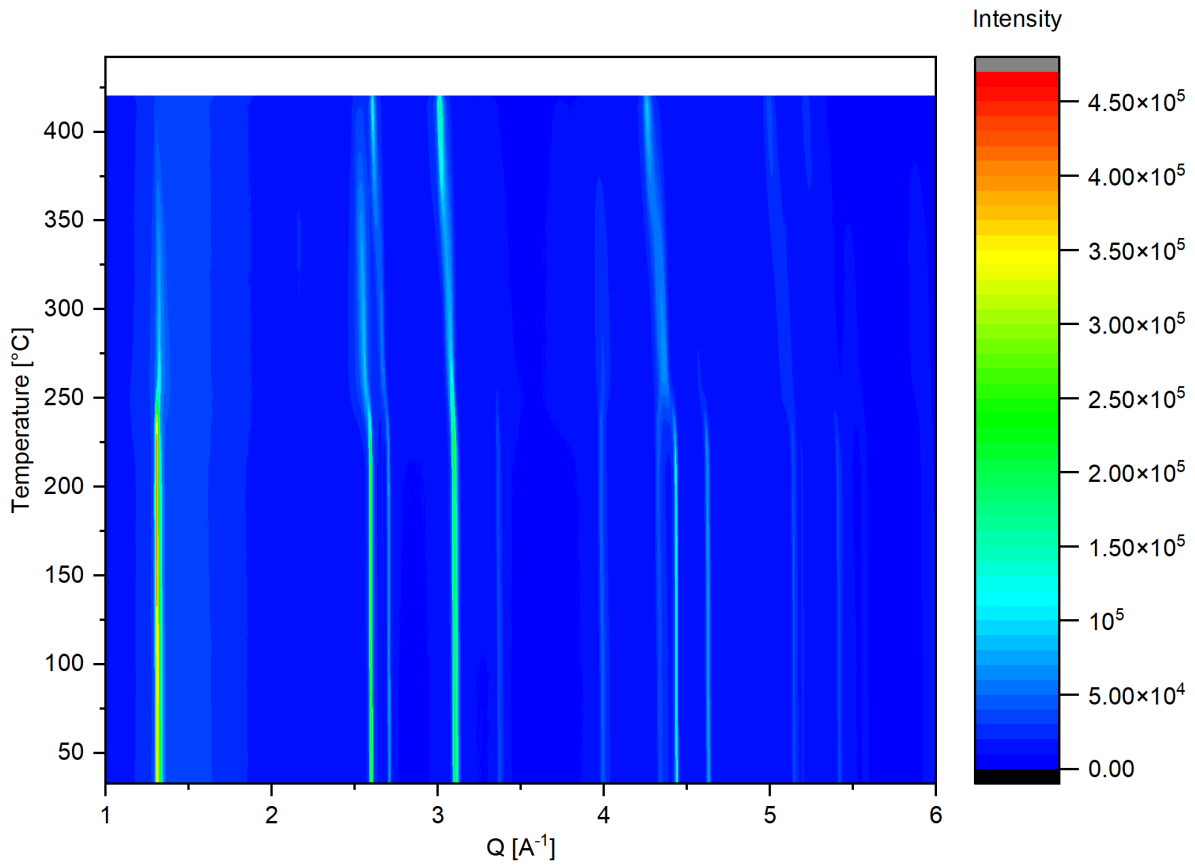

Figure S7. Diffraction patterns contour plot of delithiated annealed material. Cathode powders in a quartz capillary were heated from room temperature to 400ºC using the ITQ-ALBA capillary flow reaction cell.

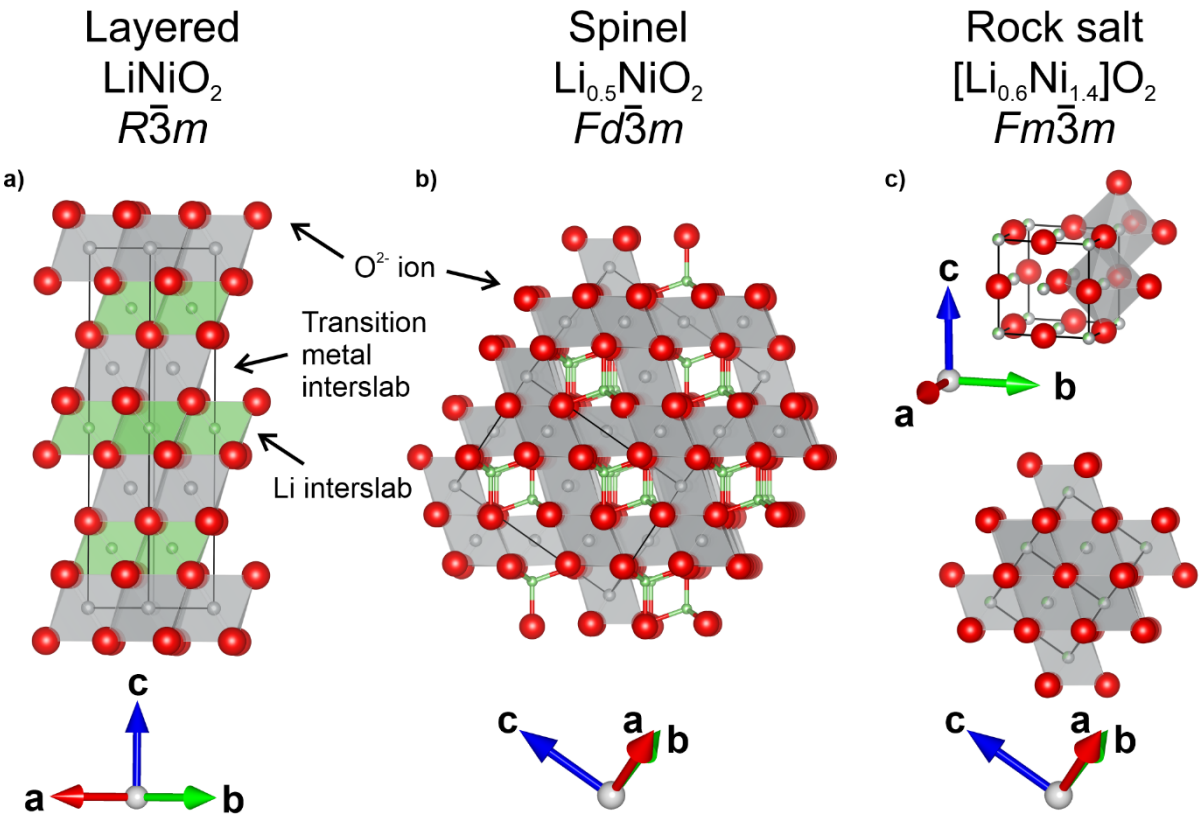

Figure S8. Comparison of the crystallographic structures with the different Li-Ni-O stoichiometries and a cubic close packing oxygen sublattice. Oxygen ions are displayed in red, Li ions are displayed in green and Ni ion are displayed in grey. For reasons of better visibility only Ni is shown as transition metal. Coordination spheres are shown either as transparent octahedra or tetrahedra as ball-stick model.

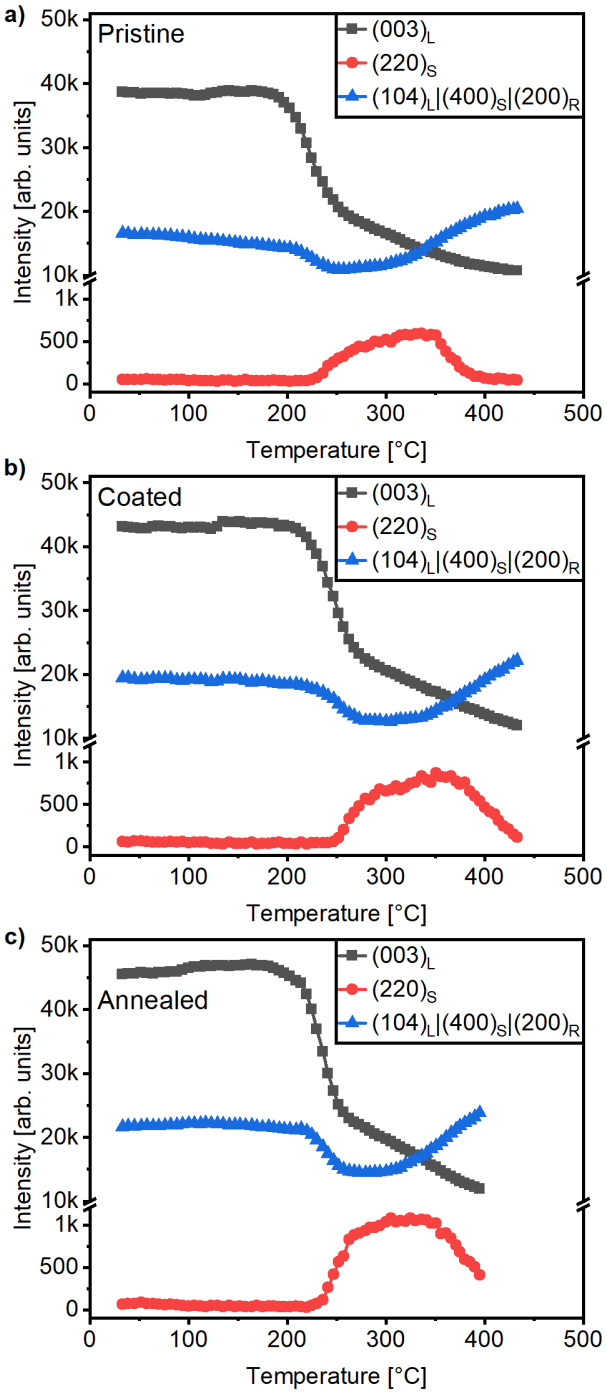

Figure S9. Phase evolutions as derived from the disappearance and appearance of selected characteristic reflections of the layered ($(003)_L$ and $(104)_L$), the spinel ($(220)_S$ and $(400)_S$) and the rock salt phases $(200)_R$.